

This article was downloaded by: [Tomsk State University of Control Systems and Radio]

On: 19 February 2013, At: 14:15

Publisher: Taylor & Francis

Informa Ltd Registered in England and Wales Registered Number: 1072954

Registered office: Mortimer House, 37-41 Mortimer Street, London W1T 3JH, UK



Molecular Crystals and Liquid Crystals

Publication details, including instructions for authors and subscription information:

<http://www.tandfonline.com/loi/gmcl16>

Low Temperature Phase Diagram of $(\text{TMTTF})_2\text{MF}_6$

R. Laversanne^a, J. Amiel^a & C. Coulon^a

^a Centre de Recherche Paul Pascal, Domaine Universitaire, 33405, TALENCE, cedex, FRANCE

Version of record first published: 13 Dec 2006.

To cite this article: R. Laversanne, J. Amiel & C. Coulon (1986): Low Temperature Phase Diagram of $(\text{TMTTF})_2\text{MF}_6$, Molecular Crystals and Liquid Crystals, 137:1, 169-178

To link to this article: <http://dx.doi.org/10.1080/00268948608070920>

PLEASE SCROLL DOWN FOR ARTICLE

Full terms and conditions of use: <http://www.tandfonline.com/page/terms-and-conditions>

This article may be used for research, teaching, and private study purposes. Any substantial or systematic reproduction, redistribution, reselling, loan, sub-licensing, systematic supply, or distribution in any form to anyone is expressly forbidden.

The publisher does not give any warranty express or implied or make any representation that the contents will be complete or accurate or up to date. The accuracy of any instructions, formulae, and drug doses should be independently verified with primary sources. The publisher shall not be liable for any loss, actions, claims, proceedings, demand, or costs or damages

whatsoever or howsoever caused arising directly or indirectly in connection with or arising out of the use of this material.

LOW TEMPERATURE PHASE DIAGRAM OF $(\text{TMTTF})_2\text{MF}_6$

R. LAVERSANNE, J. AMIELL and C. COULON
 Centre de Recherche Paul Pascal, Domaine Universitaire,
 33405 TALENCE cedex FRANCE

ABSTRACT The low temperature phase diagram of the $(\text{TMTTF})_2(\text{SbF}_6)_{1-x}(\text{AsF}_6)_x$ salts is deduced from magnetic susceptibility and antiferromagnetic resonance measurements. This phase diagram is discussed introducing a very simple model.

In addition to organic superconductivity, other low temperature ground states of organic materials have been recently studied. For example an antiferromagnetic ground state has been observed in both the TMTSF and TMTTF series^{1, 2}.

In the case of centrosymmetrical anions as MF_6 the anion ordering found for example in $(\text{TMTTF})_2\text{ClO}_4$ ³ is not expected. Nevertheless significant differences have been found in the electrical behavior of the $(\text{TMTTF})_2\text{MF}_6$ salts changing M from P to Sb. In particular the temperature dependence of the electrical conductivity shows an anomaly at 154K only in the case of the SbF_6 salt⁴. Moreover this latter compound is the only one in the $(\text{TMTTF})_2\text{MF}_6$ series presenting an antiferromagnetic ground state. On the other hand $(\text{TMTTF})_2\text{AsF}_6$ and PF_6 show Spin Peierls transitions leading to non-magnetic ground states.

The occurrence of antiferromagnetism has been previously related with the high temperature conducting behavior in the case of $(\text{TMTTF})_2\text{SCN}$. Thus it was interesting to study such a relationship in the case of centrosymmetrical anions. The high temperature electrical behavior of the $(\text{TMTTF})_2\text{MF}_6$ salts where M = P, As, Sb and the alloys P/Sb and As/Sb has been previously studied⁴. It has been assumed that the anion size was one of the main parameters driving this behavior.

In order to confirm this assumption we have performed spectroscopic and magnetic measurements on several members of this series of salts. Preliminary results concerning

mainly E.S.R. experiments have been presented at the Abano Terme conference⁵. To deepen this study we have performed magnetic measurements and antiferromagnetic resonance (AFMR) experiments. We will present in this communication the synthesis of these results and will give a qualitative discussion on the mechanism of the competition between low temperature ground states.

I. Electrical conductivity

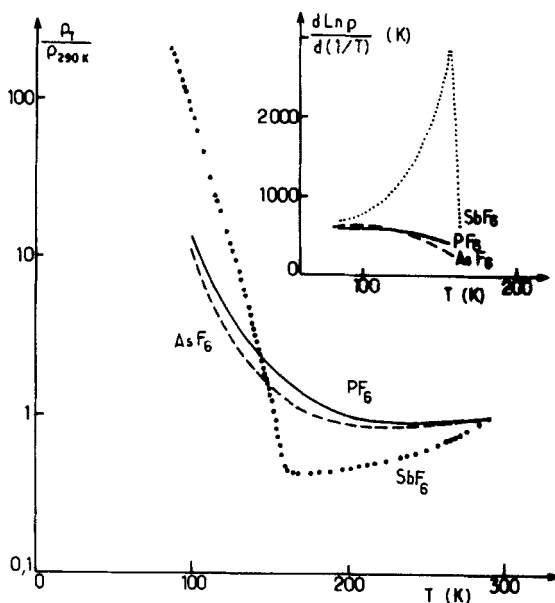


FIGURE 1 : Temperature dependence of the normalized resistivity for the three pristine salts $(TMITF)_2MF_6$. In insert is given the logarithmic derivative of the resistivity versus T .

The temperature dependence of the normalized electrical resistivity of the three salts $(TMITF)_2MF_6$ is shown figure 1. A slight minimum of the resistivity, more pronounced for the SbF_6 salt, is visible. At lower temperature the electronic localization becomes dominant and the resistivity increases rapidly particularly in the case of $(TMITF)_2SbF_6$. Moreover this salt shows an anomaly clearly visible as a sharp maximum on the derivative curve given in insert. From these results $(TMITF)_2SbF_6$ seems to be peculiar in the series.

For these three salts an exponential increase of the resistivity is found below 100K. The deduced zero Kelvin extrapolation of the gap is the same in the three cases and is about 600K. Such a value clearly demonstrates that the electrons are localized even at room temperature and the minimum of resistivity should result from a competition between the number of charge carriers and their mobility. Since a similar value of the extrapolated gap is found for the three compounds, the peculiar behavior of the SbF_6^- salt is most likely due to a sudden decrease of the charge carriers mobility.

The behavior of the SbF_6^- salt has to be related to structural results concerning the intermolecular distances. It has been found³ that the shortest distance between sulfur and fluorine decreases from PF_6^- to SbF_6^- and becomes smaller than the sum of the Van der Waals radii of the two atoms for the last anion. Consequently the interaction between the organic molecule and anion is probably stronger when the anion size increases and may be at the origin of the conductivity anomaly of $(\text{TMTTF})_2\text{SbF}_6$. One possible mechanism would be a trapping of the charge carriers induced by the freezing of the thermal motion of the anions. Within this description the origin of the electrical conductivity mechanism would be the same for the three salts although perturbations may be introduced by sufficiently big anions.

II. Low temperature ground states

Whatever is the origin of the electronic localization these salts become insulating at low temperature. Taking into account their peculiar structural arrangement (stacks of flat molecules with one transferred electron for two organic molecules : $(\text{TMTTF})_2^+\text{X}^-$) we expect at low temperature a system of localized spins with one spin per two TMTTF molecules, ie, one spin per site $(\text{TMTTF})_2^+$.

In such a system the spins are antiferromagnetically coupled and we expect two different coupling constants : J_{\parallel} for the coupling along the organic stacks and J_{\perp} for the transverse one. The anisotropy of the intra and interchain interactions is reflected in the coupling constants. J_{\parallel} is typically 100 times larger than J_{\perp} and is about a few hundred K⁶.

Antiferromagnetic coupling between spins does not always lead to a long range antiferromagnetic order. The very low values of the transverse coupling constant prevent the condensation of a three dimensional order at tempe-

ratures higher than a few K. Above this temperature the correlation length remains finite and only one dimensional fluctuations are expected.

In quasi one dimensional systems antiferromagnetic order is not the only possible ground state. In fact a one dimensional electronic chain is unstable against a structural Peierls distortion⁷. In the TMTTF series this instability leads to a dimerization of the $(\text{TMTTF})_2^+$ dimers and introduces two different longitudinal coupling constants between the spins. This dimerization produces "supersites" of four TMTTF molecules with two spins per supersite.

For the regular chains the energy of the magnetic orbitals is degenerate. The electrons remain unpaired and antiferromagnetically coupled. On the other hand in the dimerized system the overlap of magnetic orbitals preferentially occurs at the supersite. This dissymmetry splits the energy levels and removes the degeneracy. Consequently the electrons lie paired in the lowest orbital and the ground state is diamagnetic. Such a transition is of the same kind as the Peierls one and is called a Spin Peierls (SP) transition.

The two instabilities described above were shown to compete in the TMTTF series⁸. One of the parameters driving this competition is the rigidity of the lattice⁹. The structural distortion of a rigid lattice is energetically unfavorable and the antiferromagnetic order will be able to condense at low temperature. On the other hand for a soft lattice the structural distortion is energetically favoured against the AF ordering and the Spin Peierls transition will occur leading to a non-magnetic ground state.

III. Experimental results

E.S.R. experiments between room temperature and 5K on $(\text{TMTTF})_2\text{SbF}_6$ and AsF_6 were already published⁵. These results suggest an AF ground state for the SbF_6 salt and a SP transition for $(\text{TMTTF})_2\text{AsF}_6$. To deepen these points we have studied the magnetic properties of the alloys $(\text{TMTTF})_2(\text{SbF}_6)_{1-x}(\text{AsF}_6)_x$ using both susceptibility measurements and antiferromagnetic resonance.

The temperature dependence of the normalized spin susceptibility is reported figure 2 for the pure AsF_6 salt and for a few alloys close to AsF_6 . For x greater than .9 an abrupt decrease of the paramagnetic susceptibility is observed below a characteristic temperature T_C . On the other hand for x less than .8 we do not observe any anomaly above

the lowest available temperature. These experiments have been confirmed measuring the absolute magnetic susceptibility using a SQUID magnetometer with an applied field of 10 kG. Figure 3a gives the variation of the susceptibility at low temperature for $(\text{TMTTF})_2\text{AsF}_6$ and $(\text{TMTTF})_2(\text{SbF}_6)_{0.1}(\text{AsF}_6)_{0.9}$. In these two cases χ_p decreases quickly below T_C (taken as the inflexion point of the curve) to become unobservable at very low temperature as expected for a diamagnetic ground state.

Such a behavior is the signature of a Spin Peierls transition and the ground state of the alloys rich in AsF_6 is non-magnetic. The values of T_C are summarized table 1. T_C decreases rapidly when alloying to become unobservable for x less than .8.

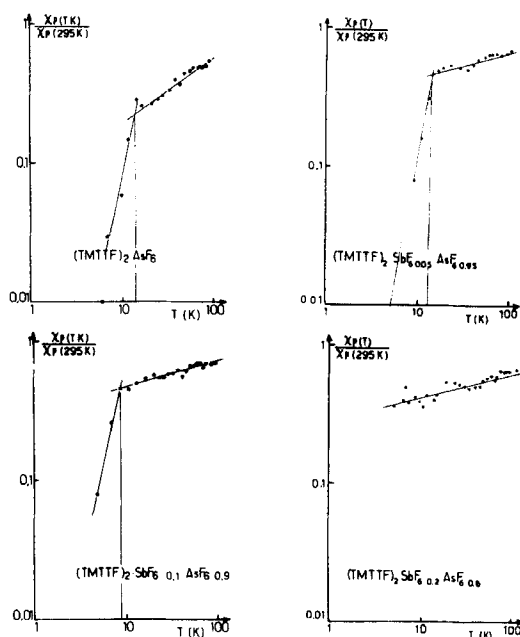


FIGURE 2 : Normalized spin susceptibility of several alloys close to $(\text{TMTTF})_2\text{AsF}_6$

On the other side (close to SbF_6) the alloys remain magnetic at very low temperature as shown by the magnetic susceptibility measurements given figure 3b. For these salts χ_p remains finite at any temperature and rises below a characteristic temperature T_N . This behavior is reminiscent of an antiferromagnetic ground state above the spin flop

field¹⁰.

A more convincing experiment is the antiferromagnetic resonance (AFMR). This method is carried out with a classical E.S.R. spectrometer and the resonance field is determined as a function of the orientation of the crystal relative to the static magnetic field.

Figure 4 gives the rotation patterns obtained for several alloys. The origin of the rotation angle is arbitrary. A shift of 90° was applied for clarity in the case of $x = 0.2$. The similarity between these rotation patterns indicates that the orientation of the magnetic axes relative to the cristallographic ones does not change noticeably when alloying. The misorientation of the magnetic axes is a consequence of the triclinic symmetry of the structure.

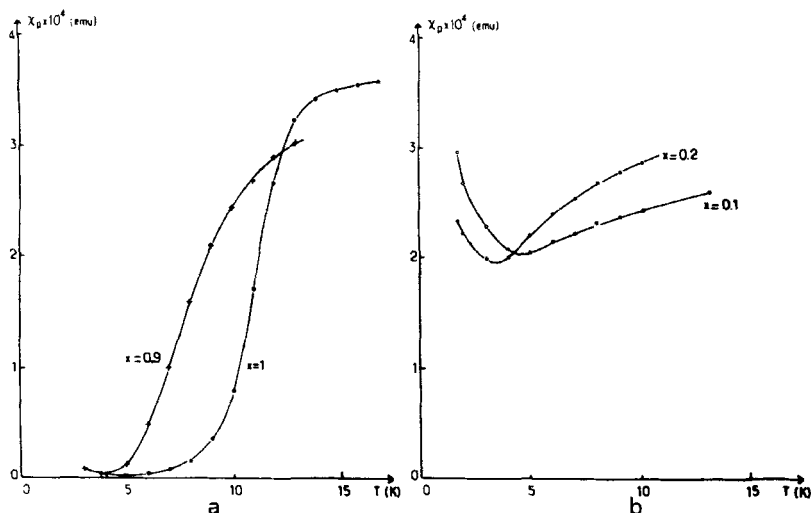


FIGURE 3 : Paramagnetic susceptibility of four members of the series with : a) $x = 1$ and $x = 0.9$
b) $x = 0.1$ and $x = 0.2$

The fits of the obtained rotation patterns (figure 4) following the NAGAMIYA¹⁰ theory were obtained taking the orientation determined for the SbF_6 salt¹¹. They give the parameters of the antiferromagnetic ground state :

- the Néel temperature T_N
- the spin-flop field H_{SF}

These parameters are summarized Table 1. Both the Néel temperature and the Spin-Flop field decrease when alloying

and for x greater than .3 T_N becomes less than our lowest available temperature.

X	0.	0.05	0.1	0.15	0.2	0.9	0.95	1.
T _C (K)						9	11.5	12.5
T _N (K)	6	5	4.6	4.1	3.5			
H _{sf} (kG)	3.3	3	2.8	2.6	2.3			

TABLE 1. Parameters of the two possible ground states for the $(TMTTF)_2(SbF_6)_{1-x}(AsF_6)_x$ salts.

IV. Low Temperature Phase Diagram

The deduced low temperature phase diagram of the $(TMTTF)_2(SbF_6)_{1-x}(AsF_6)_x$ alloys is given figure 5. The high temperature state is paramagnetic. At low temperature three cases are found depending on x . For low values of x (ie close to SbF_6) the ground state is antiferromagnetic and T_N decreases slowly when alloying. On the other side (close to AsF_6) a Spin Peierls transition occurs leading to a non-magnetic ground state. In the middle range neither of the two ground states condense and the system remains paramagnetic down to the lowest available temperature.

This experimental phase diagram has to be related to a theoretical model in which a competition between two order parameters of different symmetry is introduced. One possible topology of the corresponding phase diagram¹² is shown in insert of figure 5. Two second order lines join together at a bicritical point and the two low temperature domains are separated by a first order line. In our case P , the parameter driving the competition between the two instabilities may be related to the elasticity of the lattice⁹. This theoretical phase diagram is reminiscent of our experimental one except in the middle range where we fail to detect any three dimensional order. The origin of this difference may be the disorder induced by alloying and is illustrated using a simple schematization in the following.

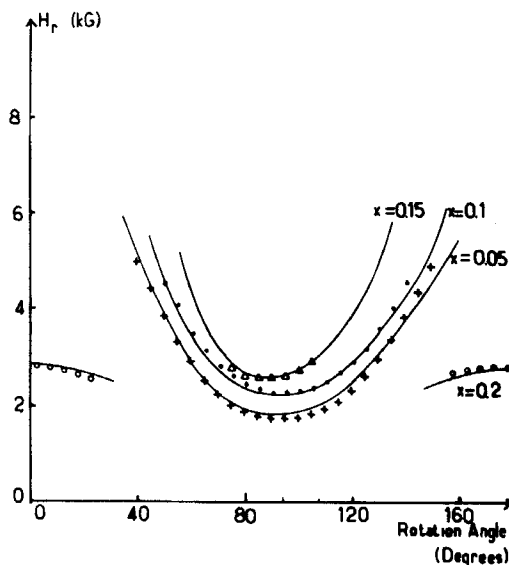


FIGURE 4 : AFMR rotation patterns about the stacking axis for four alloys with $x \leq 0.2$

Let us approximate the organic stack to a chain of sites coupled by springs. To account for the behavior of $(\text{TMTTF})_2\text{PF}_6$, the elastic constant of these springs is chosen to favor a low temperature structural distortion when the anions are weakly coupled with the organic molecules. In the case of $(\text{TMTTF})_2\text{SbF}_6$ we assumed that the anions strongly interact with the organic molecules. These interactions may enhance the elastic constant of the springs (the lattice rigidity) and consequently destabilize the structural distortion to favor the AF ground state.

Within this schematization the introduction of a few SbF_6 ions in $(\text{TMTTF})_2\text{AsF}_6$ leads to the hardening of a few springs along the chain. Thus the growth of the correlation length of the structural distortion is limited to the mean distance between locked sites. The expected consequence of this process is a decrease of the transition temperature with alloying.

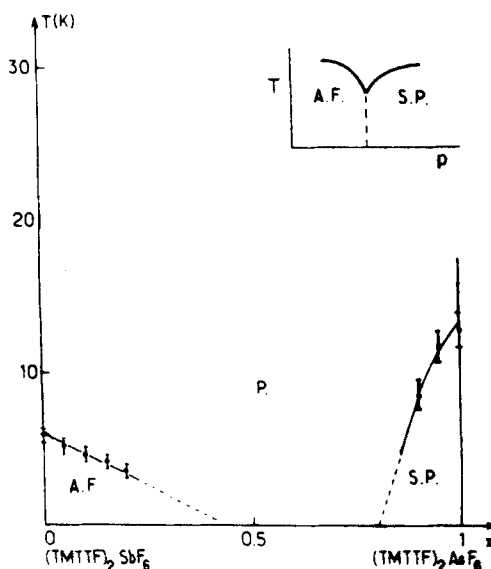


FIGURE 5 : Low temperature phase diagram of the salts $(\text{TMTTF})_2(\text{SbF}_6)_{1-x}(\text{AsF}_6)_x$. In insert is given the theoretical phase diagram mentioned in the text.

On the other hand, introducing several AsF_6 ions among the SbF_6 should be less critical for the condensation of the AF ground state which does not involve a structural distortion. The main expected effect is a renormalisation of the elastic constant of the chain leading to a smooth decrease of the Néel temperature when alloying.

In the middle range ($x \approx 0.5$) the simultaneous occurrence of these two effects may prevent the condensation of both a Spin Peierls and an AF ground state above the lowest available temperature.

Despite its simplicity, this model gives a reasonable description of the main features of the experimental phase diagram.

In summary the main conclusions of this study are the following.

First, $(\text{TMTF})_2\text{SbF}_6$ is not a singular compound in the $(\text{TMTF})_2\text{MF}_6$ series and the physical properties of the alloys are close to that of this salt for small amount of doping. Moreover the interactions between the anions and the organic stacks may be one of the driving forces to control both the electronic behavior and the competition between the low temperature instabilities. Nevertheless the disorder due to alloying should also be considered in order to describe the low temperature phase diagram.

REFERENCES

1. K. Mortensen, Y. Tomkiewicz and K. Bechgaard, *Phys. Rev. B*, **25** 3319 (1982)
S.S.P. Parkin, J.C. Scott, J.B. Torrance and E.M. Engler, *ibid*, **26** 6319 (1982)
2. C. Coulon, A. Maaroufi, J. Amiell, E. Dupart, S. Flandrois, P. Delhaes, R. Moret, J.P. Pouget and J.P. Morand, *ibid*, **26** 6322 (1982)
3. R. Moret, J.P. Pouget, R. Comes and K. Bechgaard, *J. Physique Coll.*, **44** C3 957 (1983)
4. R. Laversanne, C. Coulon, B. Gallois, J.P. Pouget and R. Moret, *J. Physique Lett.*, **45** L393 (1985)
5. R. Laversanne, J. Amiell, C. Garrigou-Lagrange and P. Delhaes, *Mol Cryst Liq Cryst*, **119** 317 (1985)
6. J.B. Torrance, *J. Physique Coll.*, **44** C3 799 (1983)
7. D. Jérôme and H.J.Schulz, *Adv. Phys.*, **31** 219 (1982)
8. C. Coulon *J. Physique Coll.*, **44** C3 885 (1983)
9. J. Kondo and T. Kinoshita, *J. Phys. Soc. Jap.*, **51** 1412 (1982)
C. Bourbonnais and L.C. Caron, *Mol. Cryst. Liq. Cryst.*, **119** 287 (1985)
10. T. Nagamiya, *Prog. Theor. Phys.*, **11** 309 (1954)
T. Nagamiya, K.Yosida and R. Kubo, *Adv. Phys.*, **4** 1 (1955)
11. C. Coulon, J.C. Scott and R. Laversanne, *Mol. Cryst. Liq Cryst*, **119** 307 (1985)
C. Coulon, J.C. Scott and R. Laversanne, *Phys. Rev. B*, *submitted*
12. J.R. Banavar, D. Jasnow and D.P. Landau, *Phys. Rev. B*, **20** 3820 (1979)